Super-expanding Chaos from the Cylinder Manifold Piecewise Linear System

Shotaro Suzuki[†] and Toshimichi Saito[†]

†Department of Electronics and Electorical Engineering, Hosei University
3–7–2 Kajino-cho, Koganei, Tokyo 184-8584, Japan
Email: shotaro.suzuki.sc@stu.hosei.ac.jp, tsaito@hosei.ac.jp

Abstract—This paper studies the chaotic dynamics of the manifold piecewise liner system on the cylinder-type phase space. This system is defined by second order continuous flow with hysteresis switching. Since the phase space is cylinder-type, the trajectories do not diverge and the system can generate super-expanding chaos characterized by a very large positive Lyapunov exponent. Using the piecewise linear 1D return map, generation of the super-expanding chaos can be analyzed theoretically.

1. Introduction

The manifold piecewise linear system (MPL) is a simple switched dynamical system that can generate chaotic attractors [1]-[3]. The MPL is defined by a second order piecewise linear system and hysteresis switching. In the history of autonomous chaotic systems, the MPL has been recognized as an important example because of the following facts. First, the dynamics is integrated into a 1D piecewise linear return map and the chaos generation [4] [5] can be proved theoretically. Second, the MPL can be implemented by a simple test circuit and chaos generation can be confirmed experimentally. Third, the MPL has been applied to engineering systems: communication systems, signal processor, radar systems, and particle swarm optimizers [6]-[10].

This paper studies the cylinder manifold piecewise linear system (CMPL). The CMPL is defined by a second-order piecewise linear system and hysteresis switching. The major difference from the MPL is the the CMPL is defined on the cylinder-type phase space. The MPL is defined in the rectangular coordinate phase space. The dynamics of the CMPL is integrated into a piecewise linear 1D return map and chaos generation can be guaranteed theoretically. Especially, it is shown that the CMPL can generate super-expanding chaos characterized by a very large Lyapunov exponent. The MPL cannot generate the super-expanding chaos.

Results of this paper can contribute to classification of chaotic phenomena and its application to engineering systems. Preliminary results can be found in [11] [12].

2. Manifold Piecewise Linear System

In this section, as a preparation, we recall the MPL presented in [1]. The MPL is defined by the following second order piecewise linear system and hysteresis switching:

$$\ddot{x} - 2\delta\dot{x} + x = \begin{cases} 1 & (+) \\ 0 & (-) \end{cases} \tag{1}$$

where x denotes the dimensionless state variable, τ denotes the dimensionless time, and $\dot{x} \equiv \frac{dx}{d\tau}$. In order to define the switching rule, we divide the x-axis L into two half lines:

$$\boldsymbol{x} \equiv (x, \dot{x}), \quad L \equiv L_+ \cup L_-$$

$$L_+ \equiv \{\boldsymbol{x} \mid x \geq Th, \ \dot{x} = 0\}, \quad L_- \equiv \{\boldsymbol{x} \mid x < Th, \ \dot{x} = 0\}$$

Switching rule of the MPL: Let the right hand side of Eq. (1) be either (+) or (−) at $\tau = 0$. The right hand side of Eq. (1) is switched from (+) to (−) if a trajectory hits L_-. The right hand side of Eq. (1) is switched from (−) to (+) if a trajectory hits L_+ (see Fig. 1).

The MPL is characterized by three parameter: the damping δ, the equilibrium point p, and the switching threshold Th. For simplicity, we assume the following case in this paper:

$$0 < \delta < 1, \quad (\omega \equiv \sqrt{1 - \delta^2}), \quad p \in \{0, 1\}, \quad Th = 0.5 \tag{2}$$

In this case, Eq. (1) has unstable complex characteristic roots $\delta \pm j\omega$. As shown in Fig. 1, the trajectories rotate divergently around equilibrium points $p \equiv \{0, 1\}$. If the trajectory hits negative x-axis (L_-) then the equilibrium point is switched from 1 to 0. If the trajectory hits positive x-axis (L_+) then the equilibrium point is switched from 0 to 1.
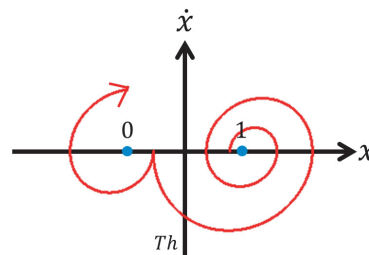

Figure 1: Trajectory of MPL for $Th = 0.5$

Note that the switching occurs only on x-axis (L). Repeating the rotation and switching, the MPL can exhibit chaotic trajectories as shown in Fig. 2 (a).

The trajectories can be calculated by the piecewise exact solution

$$x = p + (x(0) - p)e^{\delta\tau}\cos\omega\tau + \frac{1}{\omega}(\dot{x}(0) - \delta(x(0) - p))e^{\delta\tau}\sin\omega\tau, \tag{3}$$

where $(x(0), \dot{x}(0))$ is an initial condition at $\tau = 0$.

In order to define the 1D return map, we consider a trajectory started from a point $x_0 \in L$ at $\tau = 0$ where a point on L is represented by its x coordinate. The trajectory intersects L at $\tau = \pi/\omega$ and let x_1 be the intersection. Since x_0 determines x_1, we can define the 1D return map F from L to itself. The map is piecewise linear and is described exactly [1]-[3]:

$$x_{n+1} = F(x_n) \equiv \begin{cases} -\beta(x_n - 1) + 1 & \text{for } x_n \geq Th \\ -\beta x_n & \text{for } x_n < Th, \end{cases} \tag{4}$$

where $\beta \equiv e^{\frac{\delta\pi}{\omega}}$ (we will use either β or δ for convenience of explanation). Now the dynamics is integrated into the iteration $x_{n+1} = F(x_n)$. The chaos generation is guaranteed if $1 < \beta < 2$. In this case, there exists an invariant interval I_1 on which the map is expanding:

$$F(I_1) \subseteq I_1, \ |DF(x)| > 1, \ \text{for } x \in I_1 \equiv (-F(0), F(0)], \tag{5}$$

where $DF(x)$ is the slope of F at x. The map has a positive Lyapunov exponent $\ln\beta$ [3] [4]. Figure 2(b) and (d) show 1D return maps corresponding to Fig. 2(a) and (c), respectively. Note that trajectories diverge for $\beta > 2$.

3. Cylinder Manifold Piecewise Linear System

First, we define an MPL with the infinite number of equilibria (MPL$_\infty$). Introducing the cylinder-type phase space,
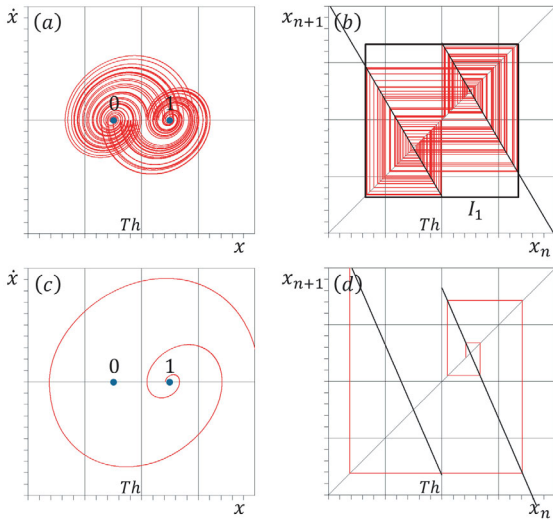

Figure 2: Trajectory and 1D return map of MPL. (a)(b) chaos for $\beta = 1.7$, (c)(d) divergence for $\beta = 2.3$.

the MPL$_\infty$ is transformed into the CMPL. The MPL$_\infty$ is defined by

$$\ddot{x} - 2\delta\dot{x} + x = p_n. \tag{6}$$

This system is characterized by three parameters δ, p_n, and T. For simplicity, we assume

$$0 < \delta < 1, \ p_n = 2nT, \ T = 0.5 \tag{7}$$

For convenience $\beta \equiv e^{\frac{\delta\pi}{\omega}}$ ($1 < \beta$).

Switching rule of the MPL$_\infty$: Let the right hand side of Eq. (6) be p_n at $\tau = 0$ and $(x, \dot{x}) \in L_0$ where

$$L_n \equiv \{\boldsymbol{x}|(2n - 1)T \leq x < (2n + 1)T, \ \dot{x} = 0\}$$

$$L = \bigcup_{n=-\infty}^{\infty} L_n, \ n = 0, \pm 1, \pm 2, \cdots,$$

The right hand side is switched to p_n if the trajectory hits L_n. The trajectory rotates around either of the equilibrium points p_n as shown in Fig. 3. If the trajectory hits L_n, the equilibrium point is switched to p_n.

Identifying L_n with L_0 for all n, the CMPL is defined. The identification is represented by

$$L_0 = G(L_n), G(X) = ((X + T)\text{mod}2T) - T. \tag{8}$$

The mapping G constructs the cylinder-type phase space. The CMPL is defined by the following.

$$\ddot{x} - 2\delta\dot{x} + x = p \tag{9}$$

Switching rule of the CMPL: Let $(x, \dot{x}) \in L_0$ at $\tau = 0$. If the trajectory hits L_n then the trajectory is switched into the L_0 as the following:

$$(x(\tau_+), \dot{x}(\tau_+)) = (G(x(\tau_+)), \dot{x}(\tau_+))$$

where τ_+ denote the time just after τ, The switching is illustrated in Fig. 4. The CMPL generates chaotic trajectories as shown in Fig. 5(a), (c), and (e).

Let us derive the 1D return map of the CMPL. Since a trajectory started from L_0 must return to L_0, the dynamics of the CMPL can be integrated into the 1D return map from L_0 to itself. The map is exactly piecewise linear and is described by

$$x_{n+1} = f(x_n) \equiv G(F(x_n)), \ F(x) \equiv -\beta(x) \tag{10}$$

Note that the domain of the map L_0 is an invariant interval: $f(L_0) \subseteq L_0$. Hence the trajectory dose not diverge as far as β is finite. This is the major difference from the MPL domain of whose return map is x-axis. Figure 5(b), (d), and (f) show examples of the return map corresponding to Fig. 5(a), (c), and (e), respectively. Since the slope of map is constant (β), the Lyapunov exponent λ of the map is $\ln\beta > 0$ [4]. Hence the CMPL generates chaos as far as β is finite. We can see that the CMPL can generate chaos with a large Lyapunov exponent $\lambda > \ln 2$. We refer to the chaos with $\lambda > \ln 2$ as the super-expanding chaos. Note that the MPL cannot generate the super-expanding chaos because the trajectories diverge for $2 \leq \beta$,
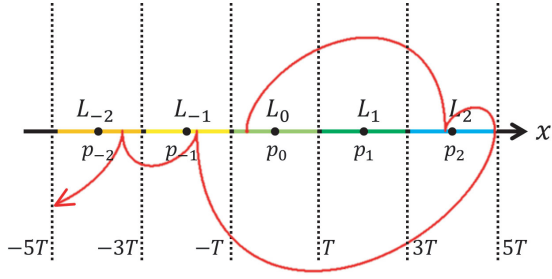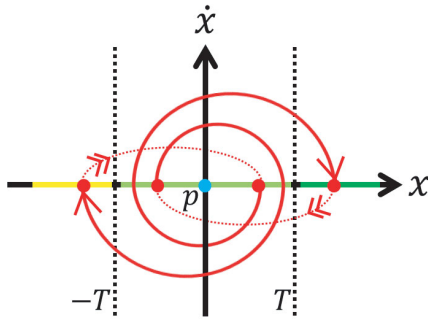
Figure 3: Switching of the MPL$_\infty$.
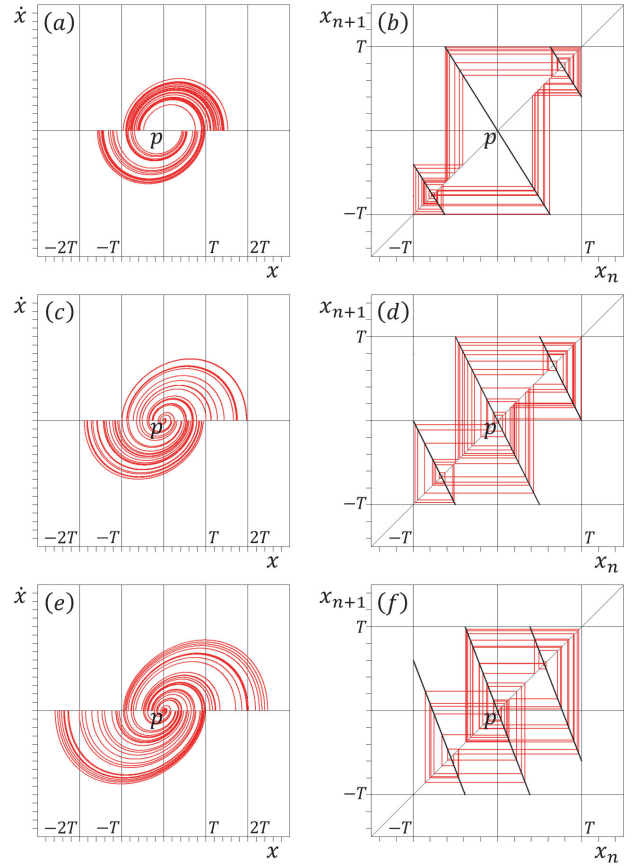

Figure 4: Switching of the CMPL

Figure 5: Trajectory and 1D return maps of the CMPL. (a) and (b) chaos for $\beta = 1.6$, (c) and (d) chaos for $\beta = 2.0$, (e) and (f) super-expanding chaos for $\beta = 2.6$.

4. Laboratory Experiments

Figure. 6(a) shows a test circuit of the CMPL. The second order circuit is fabricated by an op amps (TL072) and analog switches (TC4066). The supply voltages of the discrete elements are ±8[V]. The dynamics is described by

$$RC\frac{dv_1}{dt} = -v_2, \quad RC\frac{dv_2}{dt} = \frac{R_0}{R_2}v_2 + \frac{R_0}{R_1}v_1 \qquad (11)$$

Using the following dimensionless variables and parameters

$$\tau = \sqrt{\frac{R_0}{R_1}}\frac{t}{RC}, \quad x = \frac{v_1}{E}, \quad \dot{x} \equiv \frac{dx}{d\tau},$$

$$y = \sqrt{\frac{R_1}{R_0}}\frac{v_2}{E}, \quad 2\delta = \frac{\sqrt{R_1 R_0}}{R_2}.$$

Equation (11) is transformed into the following equation that is equivalent to Equation (9).

$$\dot{x} = -y, \quad \dot{y} - 2\delta y - x = 0 \qquad (12)$$

The second-order circuit is controlled by three kinds of switches S_1, S_2, and S_3. For simplicity, we have fabricated this circuit for the case where the switching occur in the range $-3V_B < v_1 < 3V_B$. It corresponds to the case $1 < \beta < 3$.

Figure 6(b) shows the control circuits of switches. Here, v_1 and v_2 are capacitor voltages. If $v_1 > V_B$ and $v_2 = 0$, the capacitor voltage v_1 jumps to $v_1 - 2V_B$. If $v_1 < -V_B$ and $v_2 = 0$, the capacitor voltage v_1 jumps to $v_1 + 2V_B$.

Figure 7 shows the laboratory measurements of chaotic attractors that correspond to numerical chaotic attractors in Fig. 5 (a), (c) and (e).

5. Conclusions

CMPL is presented and is analyzed in this paper. The CMPL is defined on the cylinder-type phase space and can generate the super-expanding chaos. Using the return map, the chaotic dynamics has been analyzed theoretically. Future problems include classification of chaotic attractors, laboratory measurements of various phenomena, and engineering applications.

References

[1] T. Saito and H. Fujita, Chaos in a manifold piecewise linear system, Trans. IECE, J64-A, 10, pp. 827-834, 1981 (in Japanese).

[2] T. Saito, A chaos generator based on a quasi-harmonic oscillator, IEEE Trans. Circuits Syst., 32, 4, pp. 320-331, 1985.

[3] T. Tsubone and T. Saito, Stabilizing and Destabilizing Control for a Piecewise Linear Circuit, IEEE Trans., CAS-I, 45, 2, pp. 172-177, 1998.
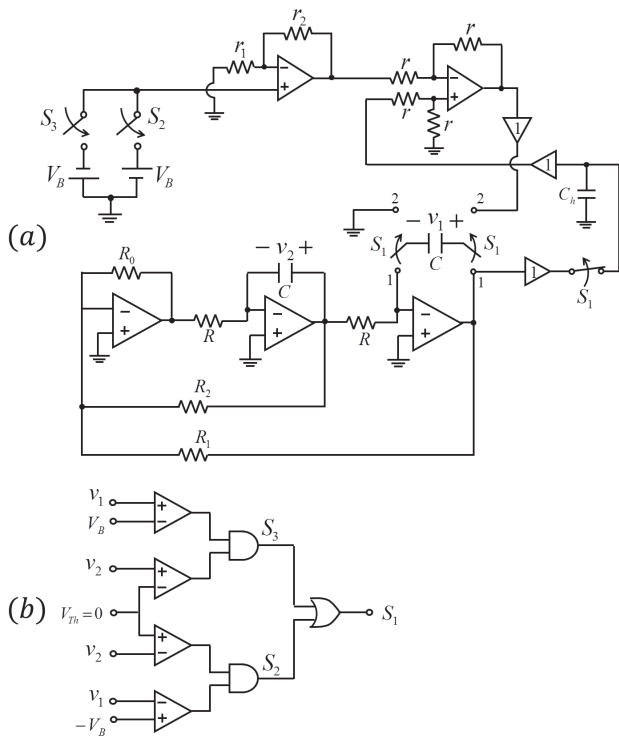
Figure 6: Test circuit of the CMPL. (a)Test circuit (b)Switching circuit

[4] A. Lasota and M. C. Mackey, Chaos, Fractals, and Noise, Springer-Verlag, 1994.

[5] S. Banerjee and G. C. Verghese, eds., Nonlinear Phenomena in Power Electronics: Attractors, Bifurcations, Chaos, and Nonlinear Control, IEEE Press, 2001.

[6] N. J. Corron, S. T. Hayes, S. D. Pethel, and J. N. Blakely, Chaos without Nonlinear dynamics, Phys. Rev. Lett., 97, 024101, 2006.

[7] N. J. Corron, J. N. Blakely, and M. T. Stahl, A matched filter for chaos, Chaos 20, 023123, 2010.

[8] N. J. Corron, M. T. Stahl, R. C. Harrison, and J. N. Blakely, Acoustic detection and ranging using solvable chaos, Chaos 23, 023119, 2013.

[9] N. J. Corron and J. N. Blakely, Exactly Solvable Chaos as Communication Waveforms Proc. of NOLTA, pp. 217-220, 2013.

[10] Y. Yamanaka and T. Tsubone, An optimizer using swarm of chaotic dynamical particles, NOLTA IEICE, 6, 1, pp. 112-130, 2015.

[11] S. Suzuki, K. Kimura, T. Tsubone and T. Saito, Manifold Piecewise Linear Chaotic System on Cylinder and Super Expanding Chaos, (V.M. Mladenov and P.C. Ivanov (Eds.): NDES 2014), CCIS 438, pp. 45-50, Springer, 2014

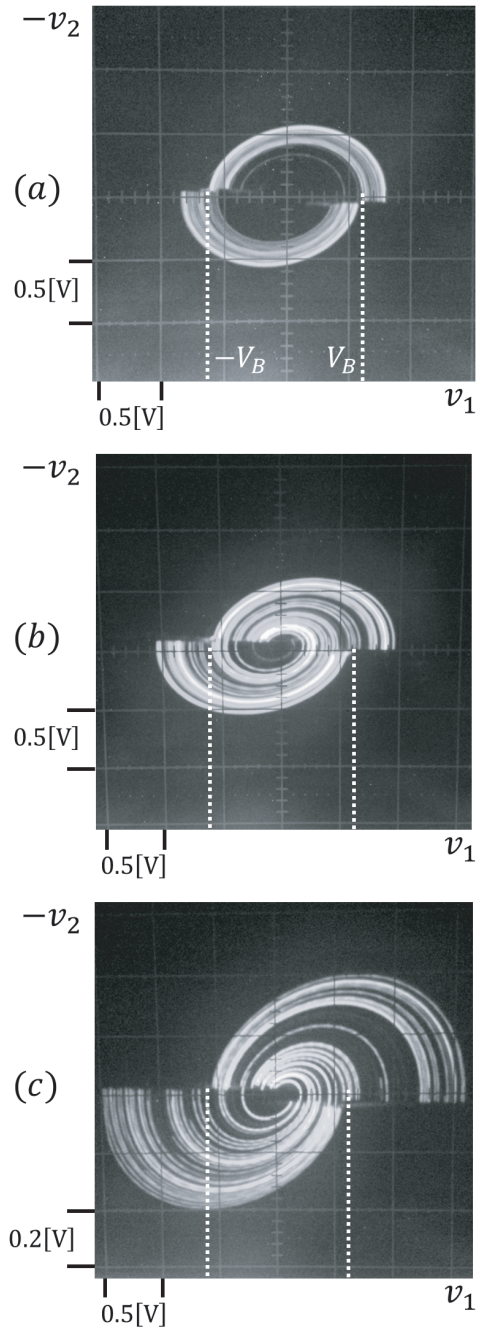[12] K. Kimura, T. Saito and T. Tsubone, An Autonomous Chaotic System on Cylinder, Proc. of NOLTA, pp. 803-806, 2014.

Figure 7: Laboratory measurements of the CMPL for $R \simeq 2[k\Omega]$, $r \simeq 1[k\Omega]$, $r_1 \simeq 3[k\Omega]$, $r_2 \simeq 3[k\Omega]$, $R_0 \simeq 1[k\Omega]$, $C \simeq 0.033[\mu F]$, $C_h \simeq 0.033[\mu F]$, $E \simeq 8.0[V]$, $V_B \simeq 0.6[V]$, (a) chaos. $R_1 \simeq 1.5[k\Omega]$, $R_2 \simeq 4.1[k\Omega]$ $\beta \simeq 1.6$. (b) chaos. $R_1 \simeq 2.8[k\Omega]$, $R_2 \simeq 3.8[k\Omega]$ $\beta \simeq 2.0$. (c) super-expanding chaos. $R_1 \simeq 7.5[k\Omega]$, $R_2 \simeq 4.5[k\Omega]$ $\beta \simeq 2.6$